



AN ABSTRACT OF THE THESIS OF

Mark Charles Williams for the degree of Master of Science in Geophysics  
presented on July 1, 2011.

Title: Seismicity at the Cascadia Plate Boundary Beneath  
the Oregon Continental Shelf

Abstract approved: \_\_\_\_\_

Anne M. Tréhu

Since 2003, 39 small earthquakes have been detected offshore central Oregon in the nominally locked part of the Cascadia subduction zone, where very little seismic activity has been recorded in spite of a paleo-seismic record of great subduction events. Although the regional earthquake bulletin reports depths of 29 and 28 km for the two largest events ( $M_w$  4.9 and  $M_w$  4.7, which occurred in 2004), analysis by *Tréhu et al.* (2008) indicates that they were low angle thrust events that occurred on the plate boundary at depths of 9-11 and 16 km, respectively. Due to sparse onshore station coverage, most of the smaller events have large location uncertainties. Double-difference relative location of 30 of these earthquakes reveals two tight clusters approximately 30 km apart; each cluster is associated with one of the two larger events. Within each cluster, relocation reduces the hypocenter depth spread from  $> 15$  km to  $< 3$  km, with uncertainties on the order of 0.1 km. The relocations, combined with independent absolute hypocenter locations for two 2008 events using a deployment of land and ocean bottom seismometers, suggest that the seismicity occurred at plate boundary depths, possibly on the Cascadia megathrust. This con-

centrated activity in the seismogenic zone may represent patches on the fault plane with anomalous frictional characteristics, possibly caused by subducted topographic features, which can affect the propagation of a large megathrust rupture.

©Copyright by Mark Charles Williams

July 1, 2011

All Rights Reserved

Seismicity at the Cascadia Plate Boundary Beneath the Oregon Continental Shelf

by

Mark Charles Williams

A THESIS

submitted to

Oregon State University

in partial fulfillment of  
the requirements for the  
degree of

Master of Science

Presented July 1, 2011  
Commencement June 2012

Master of Science thesis of Mark Charles Williams presented on July 1, 2011

APPROVED:

---

Major Professor, representing Geophysics

---

Dean of the College of Oceanic and Atmospheric Sciences

---

Dean of the Graduate School

I understand that my thesis will become part of the permanent collection of Oregon State University libraries. My signature below authorizes release of my thesis to any reader upon request.

---

Mark Charles Williams, Author

## ACKNOWLEDGEMENTS

Firstly, I would like to thank my adviser, Anne Tréhu, for all of her support during my time here. Anne is a tireless advocate in her field and for science in general, and she has not only shared her experience and enthusiasm, but has also always encouraged me to develop my own thoughts and ideas.

Thanks to Jochen Braunmiller, John Nabelek, and Andrew Meigs for serving on my committee, and more importantly, for the many hours of formal and informal education I have received from all of them over the years, in the classroom, in the lab, and especially in the field. They were (and still are) always willing to sit down and explain the finer points of geophysics to an electrical engineering major.

The entire Marine Geology and Geophysics faculty, as well as the broader faculty of COAS, have taught, helped, and supported me over the years, including Rick Vong, Jeff Barnes, and the administration and staff of the college.

Also many thanks are due to my fellow graduate students in the Seismic Imaging Laboratory: Peter, Patrick, and Evan, for helping, entertaining, and putting up with me on a daily basis, as well as the all the other graduate students in COAS, including the Snack Lunch group.

I have had the privilege of playing with many fine musicians during my time in Oregon, but special thanks go to Kevin Groh, Dustin Herron, Joshua Kitner, Ezra Markowitz, Corey Murphy, Daniel Scharp, and James Wilson, who, for a short time, were my family away from home and helped me in countless ways.

Lastly, none of this would have been possible without the love and support of my parents, Donald and Anne, my siblings, Christina, Janet, and Matthew, and the rest of my family. Thank You.

## CONTRIBUTION OF AUTHORS

Dr. Tréhu was the Principal Investigator of the COLZA experiment, which consisted of seismic stations used in this study. Dr. Tréhu and Dr. Braunmiller assisted in the interpretation of the relocation data and its implications.

## TABLE OF CONTENTS

	<u>Page</u>
1. INTRODUCTION .....	1
1.1. Earthquakes in Cascadia .....	1
1.2. Organization of the Manuscript .....	2
2. SEISMICITY AT THE CASCADIA PLATE BOUNDARY BENEATH THE OREGON CONTINENTAL SHELF .....	4
2.1. Introduction .....	5
2.2. Data and Methods .....	7
2.3. Relocations and Analysis .....	13
2.3.1 Absolute cluster depth location .....	14
2.3.2 Location of two earthquakes with COLZA stations .....	14
2.3.3 Relative Relocations .....	17
2.4. Discussion .....	20
2.5. Conclusions .....	23
2.6. Data and Resources .....	24
2.7. Acknowledgements .....	24
3. CONCLUSIONS .....	26
3.1. Suitability of the hazard earthquake catalog for offshore scientific research .....	26
3.2. Co-located static and kinematic evidence for frictional anomalies ..	26
3.3. Possible implications for rupture segmentation .....	27
BIBLIOGRAPHY .....	28

## LIST OF FIGURES

<u>Figure</u>	<u>Page</u>
2.1 Map of area .....	7
2.2 Magnitude vs. time plot for earthquakes in the region of study .....	8
2.3 Waveforms and correlation matrix example .....	12
2.4 Weighted rms error for hypoDD relocation .....	13
2.5 Absolute depth location results .....	16
2.6 Before and after epicenter maps .....	18
2.7 Depth relocation cross-sections .....	19
2.8 Final event locations with velocity model .....	21

## LIST OF TABLES

<u>Table</u>	<u>Page</u>
2.1 Earthquakes used in relocation .....	9
2.2 Stations with picked arrivals used in hypoDD.....	10

# SEISMICITY AT THE CASCADIA PLATE BOUNDARY BENEATH THE OREGON CONTINENTAL SHELF

## 1. INTRODUCTION

### 1.1. Earthquakes in Cascadia

In the Pacific Northwest of North America, there exists the potential of significant damage from the natural hazards of both earthquakes and volcanoes related to the Juan de Fuca tectonic plate subducting beneath the continent. The coastal areas are also subject to tsunami generated from local and distant sources. The Cascadia subduction zone, along the western edge of the North American continent, is one of six regions on the Earth capable of producing an earthquake of magnitude 9 or greater. For this reason, it has been the subject of extensive scientific study. However, because the last great earthquake in Cascadia occurred before the age of modern seismographs, little is known about the mechanism and behavior of a large megathrust earthquake rupture in this region. Evidence of past ruptures is historical, and restricted to what has been preserved in the natural record. In order to better mitigate damage, improve forecasting, and learn from future earthquakes, the emphasis of study in Cascadia from an earthquake hazard perspective has been on gathering data on past large earthquakes and recently, studying present related phenomena, such as slow slip.

The exact nature of the frictional properties that control a large earthquake's initiation, propagation, and eventual termination is an ongoing subject of study in the field of geophysics. Effects of temperature and pressure on the elastic and rheological properties of the lithosphere are not well understood, especially at seismogenic plate boundary depths. Displacement and strain measurements taken near the surface must be projected to the plate boundary. Therefore earthquakes themselves are valuable evidence of *in situ* behavior on an active fault, and aside from active source imaging, can be the best indicator of fault structure at depth.

In the following manuscript, small to medium sized earthquakes occurring in clusters offshore of Cascadia are relocated in order to reduce the location uncertainty and ultimately produce more accurate and precise locations. These new locations are then briefly discussed in the context of existing datasets of the region, including active source seismic, magnetic, gravity, and GPS surveys.

While smaller magnitude earthquakes are observed at the plate boundaries of other subduction zones around the world, the seismogenic zone at Cascadia, especially the central portion spanning southern Washington state and Oregon, has been relatively quiescent. The small-scale, focused seismicity in this manuscript is somewhat unique in this area and provides not only some small insights into micro-earthquakes, but also has possible implications and value in the event of a large earthquake in the future.

## **1.2. Organization of the Manuscript**

This thesis consists of a manuscript subjected to peer review and accepted for publication in the Bulletin of the Seismological Society of America. The abstract

and references of the paper have been incorporated into the appropriate sections of the thesis. The remainder of the manuscript is reproduced as accepted by the journal, and as such, has its own Introduction, Methods, Discussion, and Conclusion sections.

## 2. SEISMICITY AT THE CASCADIA PLATE BOUNDARY BENEATH THE OREGON CONTINENTAL SHELF

Mark C. Williams, Anne M. Tréhu, and Jochen Braunmiller

Bulletin of the Seismological Society of America

Published by: Seismological Society of America, 201 Plaza Professional Building,  
El Cerrito, California, 94530

Vol. 101, No. 3, pp. 940-950, June 2011, doi: 10.1785/0120100198

## 2.1. Introduction

The Juan de Fuca plate subducts beneath North America at the Cascadia Subduction Zone. While no large subduction megathrust earthquake has been recorded in Cascadia, there is a large amount of historical and paleo-seismic evidence that great earthquakes and their resulting tsunamis have occurred in this region. Based on evidence of an “orphan” tsunami in Japan, the last great earthquake in Cascadia occurred in January 1700 (*Satake et al.*, 2003; *Atwater*, 2005). Records of coastal co-seismic subsidence (*Leonard et al.*, 2003; *Nelson et al.*, 2006) and offshore turbidite sequences (*Adams*, 1990; *Goldfinger et al.*, 2003) indicate that the margin has ruptured numerous times in the past. Moreover, along-strike variability of these records implies that partial ruptures, as well as ruptures of the entire margin, have occurred. This behavior is observed in other subduction zones as well. In fact, this may be a common characteristic of subduction zones capable of  $M > 9$  earthquakes. The model of a magnitude 9+ earthquake as a continuous rupture of adjacent “locked” patches relates to a fundamental seismological question: what controls the frictional regime that causes termination or continuation of rupture in a great earthquake?

In 2004, two moderate-sized earthquakes ( $M_w$  4.9 on 07/12/04 and  $M_w$  4.7 on 08/19/04) occurred in the nominally “locked” or “transitional” portion of the subduction zone. These events were of interest because the epicenters were located at the edge of a rupture segment proposed by paleo-seismic estimates of past megathrust ruptures (*Goldfinger et al.*, 2008). *Tréhu et al.* (2008) determined that both earthquakes were low-angle thrust events. Moreover, the initial catalog locations were too deep to produce observed PmP and pP phases. By tracing rays through a

2-D velocity model grid of possible source locations, they concluded the events were at depths of 9-11 and  $\sim 16$  km and likely occurred on the plate boundary, which had been previously determined based on active source seismic work (*Tréhu et al.*, 1994; *Gerdom et al.*, 2000).

In addition to these two moderate events, 37 smaller earthquakes in this area have been detected by regional networks between 2003 and 2008. We used a double-difference algorithm, hypoDD (*Waldhauser and Ellsworth*, 2000), to precisely relocate these events relative to each other. Because of the 1-D velocity model used by the algorithm, absolute locations produced by hypoDD are subject to a significant bias (as are the catalog locations), dependent mainly on the absolute starting depth. The analysis of the two larger events by *Tréhu et al.* (2008), as well as the independent location of 2 offshore events captured by our amphibious array, are used to verify our choice of starting location (epicenter and depth) in hypoDD. Focal mechanisms for the two larger events, clusters of relocated events, and nearby stations are mapped in Figure 2.1.

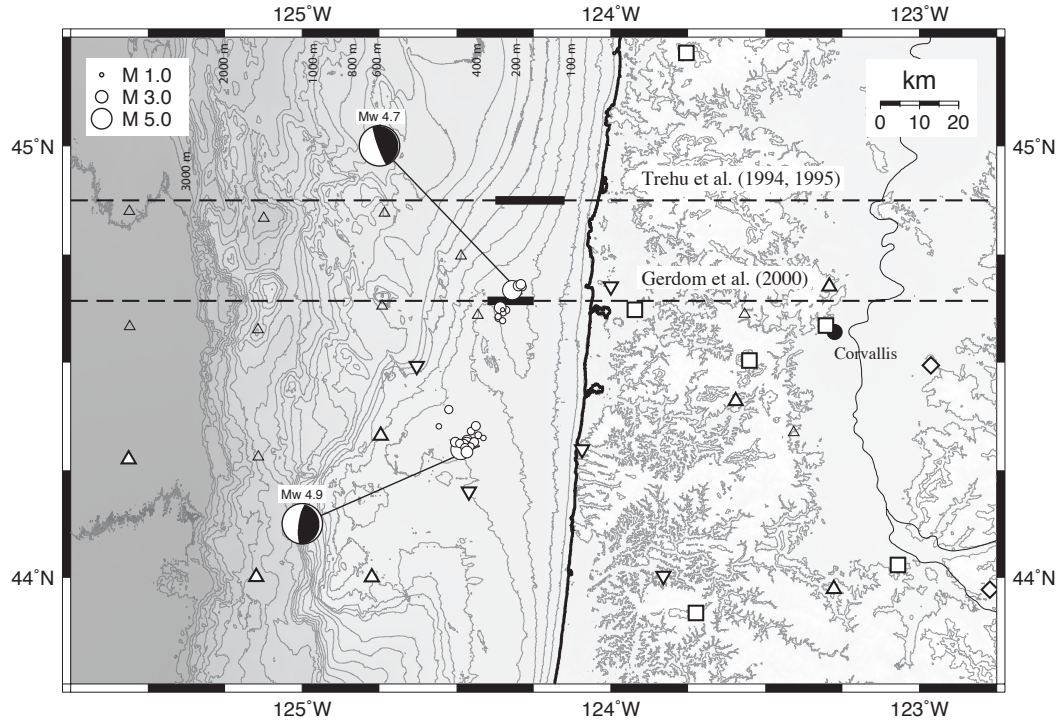


FIGURE 2.1: Map of area showing final relocated earthquake epicenters (circles) and seismic stations, including permanent stations (squares), temporary stations (triangles), and borehole seismometers (diamonds). Large white symbols are stations used for hypoDD locations; five stations (inverted triangles) were also used to compute two absolute locations of events in the southern cluster. Not all stations were deployed during the entire period of seismicity (see Table 2.2). Focal mechanisms are from *Tréhu et al. (2008)*. Dashed lines are seismic lines by *Tréhu et al. (1994, 1995)*; *Gedom et al. (2000)*; solid line portion of the seismic surveys are spots of high reflectivity on the subducting plate.

## 2.2. Data and Methods

We identified 39 events occurring from 2003 to 2008 in the area from 44° to 45°N and 125° to 124°W. Figure 2.2 gives a magnitude-time plot of events, which are listed in Table 2.1. The earthquakes were extracted from the Pacific Northwest

Seismic Network (PNSN) and the EarthScope USArray Network Facility (ANF) catalogs. Five smaller earthquakes in 2006 were not detected by the PNSN; the densely spaced USArray TA stations detected these events, resulting in a more complete offshore micro-earthquake catalog.

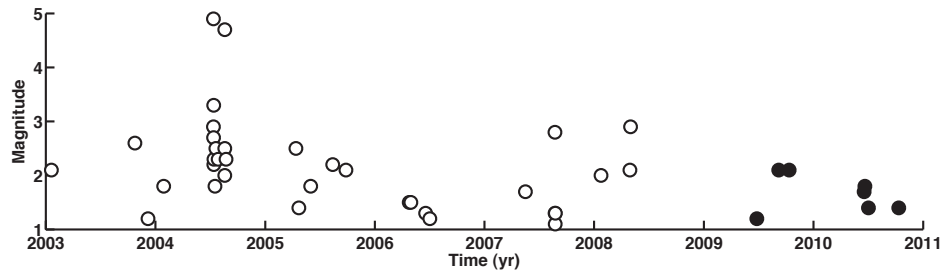


FIGURE 2.2: Magnitude vs. time plot for earthquakes occurring in the region of study from 2003 through 2010. Several small earthquakes per year have been occurring in this region since the M 4.9 and 4.7 events in 2004. Magnitudes for earthquakes in 2006, detected by ANF only, are estimated by comparing waveform amplitude to other events with known PNSN magnitude. Earthquakes occurring after 2009 have minimal station coverage overlap with events from 2007 to 2008 and were not included in this study.

We collected waveforms from the PNSN stations, the EarthScope USArray (TA), Plate Boundary Observatory borehole seismic network (PBO), Central Oregon Locked Zone Array (COLZA) FlexArray stations, and the Global Seismic Network (GSN) station COR. Prior to 2005 only COR and PNSN stations were operating in the region. Only seven permanent sites, installed prior to 2003, provide waveforms for all events. Station coordinates and recording time periods are given in Table 2.2 to document the changing recording configuration.

Catalog locations for the smaller events broadly cluster around the two larger events, with depths ranging from 15 to 35 km. However, waveform similarity, combined with S-P arrival times, suggests the smaller events are not distributed throughout the region, but occurred very close to the two M $\sim$ 5 earthquakes. Figure 2.3 shows normalized vertical component waveforms for events picked at station COR,

## Earthquakes Selected from Regional Catalogs between 2003 and 2008

ID	Date	Time	Latitude	Longitude	Depth	Mag	Nst	Nph	Networks
1	1/19/2003	22:00:32.80	44.3912	-124.5258	13.04	2.1	7	11	IU UO UW
2*	10/25/2003	02:08:54.89				2.6	5	8	IU UO UW
3	12/7/2003	17:37:36.35	44.6238	-124.3469	17.17	1.2	5	9	IU UO UW
4	1/28/2004	23:03:42.30	44.6211	-124.3397	16.93	1.8	6	9	IU UO UW
5*	2/6/2004	06:12:36.10	-	-	-	2.4	6	8	IU UO UW
6*	3/21/2004	22:35:08.90	-	-	-	2.2	3	4	IU UW
7	7/12/2004	16:41:19.24	44.2968	-124.4901	12.14	2.9	8	12	IU UO UW
8	7/12/2004	16:44:59.34	44.2977	-124.4869	12.92	4.9	8	13	IU UO UW
9	7/13/2004	00:26:31.43	44.3180	-124.4658	12.90	2.7	8	11	IU UO UW
10	7/13/2004	03:56:11.61	44.3115	-124.4676	13.03	3.3	8	12	IU UO UW
11	7/13/2004	15:00:36.93	44.3150	-124.4431	13.07	2.2	4	6	IU UW
12	7/14/2004	07:44:37.88	44.3153	-124.5040	12.04	2.3	5	9	IU UO UW
13	7/17/2004	14:54:55.92	-	-	-	1.7	5	7	IU UO UW
14	7/17/2004	16:54:53.64	44.3406	-124.4537	11.89	1.8	4	6	IU UO UW
15	7/20/2004	15:58:48.67	44.3051	-124.4675	11.96	2.5	6	10	IU UO UW
16	7/27/2004	23:28:27.18	44.3101	-124.4765	12.02	2.3	6	12	IU UO UW
17	8/19/2004	06:06:03.92	44.6677	-124.3201	18.09	4.7	7	13	IU UO UW
18	8/19/2004	06:26:00.03	44.6751	-124.2882	18.23	2.0	6	9	IU UO UW
19	8/19/2004	07:54:10.71	44.6781	-124.2995	18.85	2.5	6	12	IU UO UW
20	8/23/2004	08:04:44.36	44.6811	-124.2927	18.52	2.3	6	11	IU UO UW
21*	4/13/2005	04:51:05.92	-	-	-	2.5	6	10	IU UO UW
22*	4/23/2005	01:38:01.91	44.3517	-124.5581	14.34	1.4	5	7	IU UO UW
23	6/1/2005	07:20:00.92	44.3048	-124.4560	10.64	1.8	5	8	IU UO UW
24	8/13/2005	17:41:13.42	44.3528	-124.4381	13.93	2.2	6	8	IU UO UW
25*	9/26/2005	18:11:04.97	-	-	-	2.1	6	10	IU UO UW
26*	4/25/2006	06:56:35.00	-	-	-	1.5†	10	14	IU TA UO UW
27	5/1/2006	04:10:14.17	44.6022	-124.3656	16.42	1.5†	9	14	IU TA UO UW
28*	6/14/2006	14:16:22.00	-	-	-	n/d	5	5	TA UW
29	6/19/2006	00:53:54.85	44.6064	-124.3659	16.62	1.3†	5	10	IU TA UW
30	7/3/2006	04:45:15.48	44.5969	-124.3513	17.09	1.2†	5	9	IU TA UW
31*	4/8/2007	09:34:32.42	-	-	-	1.8	14	21	IU PB TA UO UW
32	5/17/2007	09:35:09.43	44.3307	-124.4300	12.53	1.7	10	16	IU TA UO UW
33	8/23/2007	22:31:00.35	44.6269	-124.3584	17.13	2.8	12	19	IU TA UO UW
34	8/24/2007	03:30:24.24	44.6144	-124.3490	16.99	1.3	10	16	IU PB TA UW
35	8/24/2007	12:22:39.69	44.6220	-124.3516	16.72	1.1	13	21	IU PB TA UO UW
36	8/25/2007	01:09:41.60	44.3245	-124.4136	13.17	1.3	9	13	IU PB TA UW
37	1/24/2008	09:40:41.88	44.3118	-124.4903	10.70	2.0	18	30	IU TA UO UW XA
38	4/29/2008	17:18:45.47	44.3022	-124.4734	13.69	2.1	19	34	IU PB UO UW XA
39	5/1/2008	16:20:44.37	44.2923	-124.4666	13.04	2.9	22	38	IU PB UO UW XA

TABLE 2.1: These events were selected from the regional catalogs of PNSN and ANF. Hypocenters of relocated earthquakes are listed, including the number of stations and phases for which arrivals were picked. For non-relocated events, the catalog date and time are listed. An asterisk (\*) denotes ID numbers of earthquakes that were not relocated. A dagger (†) denotes magnitudes estimated by waveform comparison with similar events of known magnitude; these events were detected by ANF, which does not report magnitude.

Stations used for locations

Net	Sta	Ondate	Offdate	Lat	Lon	Elev
IU	COR	1995133	-	44.5855	-123.3046	0.110
PB	B026	2007055	-	45.3094	-123.8230	0.107
PB	B028	2007078	-	44.4937	-122.9638	0.140
PB	B030	2007295	-	43.9713	-122.7717	0.264
PB	B031	2007334	-	43.6643	-123.3967	0.689
PB	B032	2007336	-	43.6680	-123.3923	0.064
PB	B033	2007347	-	43.2917	-123.1245	0.312
TA	I02A	2005321	-	44.0035	-123.8299	0.170
TA	I03A	2005322	-	43.9726	-123.2777	0.206
TA	G03A	2006196	-	45.3153	-123.2811	0.208
TA	H02A	2005319	-	44.6764	-123.9997	0.209
TA	H03A	2005314	-	44.6765	-123.2923	0.214
TA	J03A	2005349	2007304	43.3717	-122.9646	0.292
TA	J02A	2005320	-	43.3654	-123.5747	0.136
UO	DBO	1994032	-	43.1190	-123.2439	0.984
UO	EUO	2001108	-	44.0292	-123.0701	0.160
UW	HEBO	2001304	-	45.2135	-123.7554	0.875
UW	MPO	1990242	-	44.5047	-123.5514	1.249
UW	RNO	1991268	-	43.9162	-123.7250	0.850
UW	TOLO	2001296	-	44.6219	-123.9225	0.021
XA	ALS0	2008023	2009365	44.4104	-123.5952	0.315
XA	MAP0	2008025	2009365	44.0035	-123.8298	0.143
XA	TOL0	2008023	2009365	44.6764	-123.9997	0.191
XA	YAC0	2008022	2008137	44.2982	-124.0932	0.320
XA	OBS07	2007250	2008189	44.6313	-124.7412	-0.270
XA	OBS09	2007252	2008189	44.2755	-125.5627	-2.985
XA	OBS12	2007251	2008189	44.2000	-124.4597	-0.097
XA	OBS14	2007251	2008189	44.0010	-125.1490	-1.531
XA	OBS15	2007251	2008189	44.0002	-124.7748	-0.123
XA	OBS16	2007251	2008189	44.4917	-124.6289	-0.163

TABLE 2.2: Stations with picked arrivals used in hypoDD

divided into northern and southern clusters, accompanied by correlation matrices. The strong similarity between some groups of events suggests not only close spatial proximity, but also a similar source mechanism.

We manually picked P and S arrivals for all 39 events and assigned an arrival time uncertainty for each pick. The uncertainties were binned into weights and entered into hypoDD. At some stations, small events were not recorded well enough to pick distinct arrivals accurately. Two events were *a priori* excluded due to lack of arrival information; seven events that lacked a sufficient number of arrivals, or produced unrealistic residuals (reflecting large pick uncertainties at noisy stations) were not relocated by hypoDD based on user specifications. Our arrival-time dataset also includes cross-correlation P arrival time differences. Cross-correlations were calculated over 2-second windows around the P arrival in the frequency domain, using the method of West (see Data and Resources). Weights for the differential times are based on the correlation value and are used as *a priori* weights for those inputs. During hypoDD iterations, the cross-correlation data are weighed based on inter-event distance, and used only between pairs of events within the same cluster. Table 2.1 shows the entire catalog of events, including number of stations, picks, and networks used in the relocation.

Using the hypoDD algorithm and a velocity model derived from *Gerdom et al.* (2000), we ran a relocation consisting of 4 sets of iterations (31 iterations total). Each set of iterations utilized a different weighting scheme that progressively up-weighted data for event pairs that were closer to one another, and preferentially used cross-correlation data for event pairs within a distance of 2 km (for details on the weighting approach see *Waldhauser and Ellsworth* (2000)). The root mean squared (RMS) residual was calculated separately for both the manually picked data and

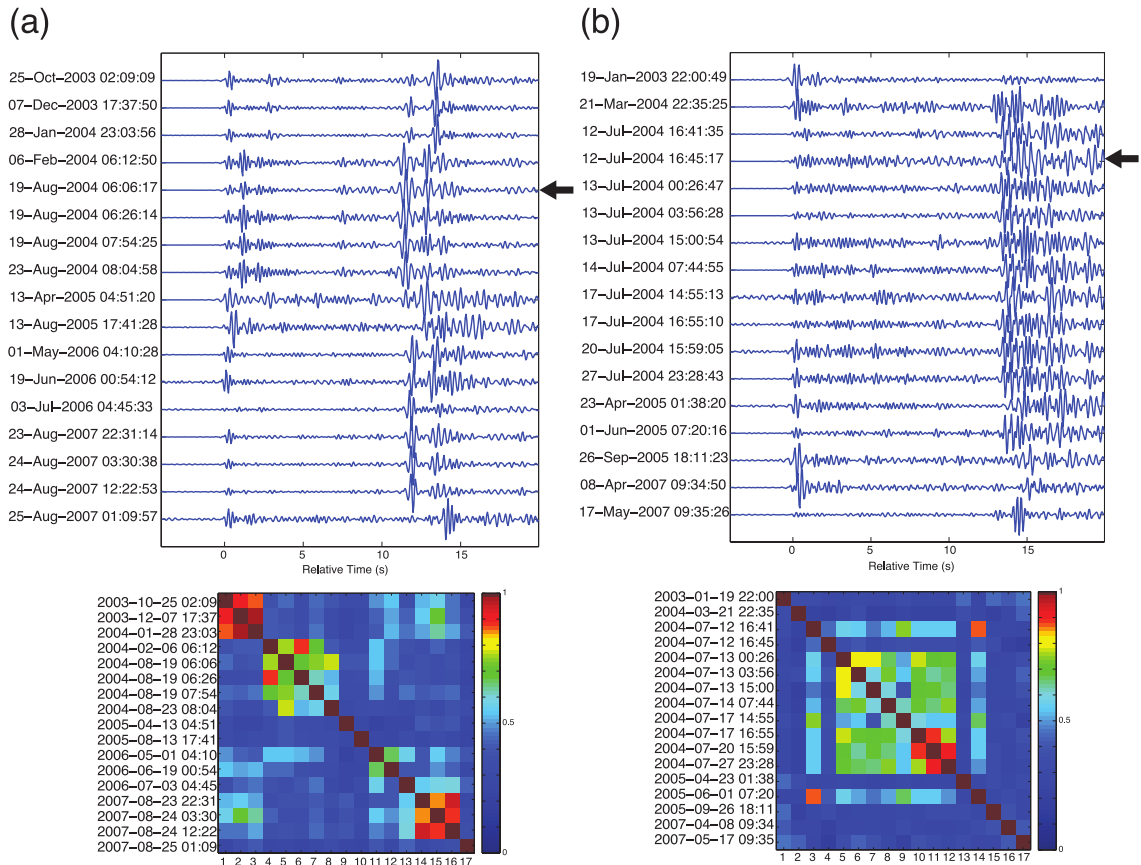


FIGURE 2.3: Waveforms and correlation matrices for picked events on the vertical channel at station COR for (a) northern cluster and (b) southern cluster earthquakes. Waveforms are normalized and filtered from 2 to 5 Hz, aligned to first arrival. The largest event in each cluster is indicated by an arrow. Note the waveform similarity in (a) between the main event and the subsequent aftershocks, and in comparison, the similarity within the 2003, 2006, and 2007 event group. These two groups of earthquakes are distinctly separated in the relocation. Southern cluster events in (b) have similar S–P times, but larger waveform variability.

the cross-correlation data, and we considered that the solution had converged when the RMS for each dataset was below 0.1 and stable. Figure 2.4 shows the residual of each dataset as a function of iteration. The sharper drops in residual reflect the points at which a more selective weighting scheme was implemented. At the end of the relocation process, there were 30 earthquakes with sufficient event-pair data to

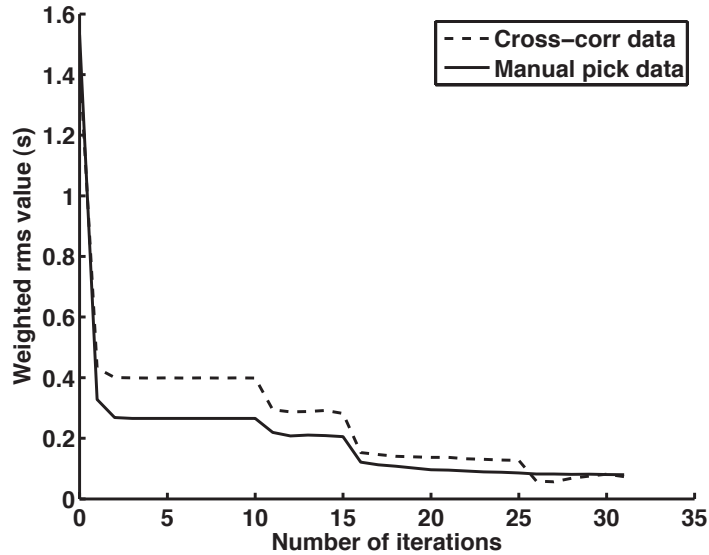


FIGURE 2.4: Weighted rms error as a function of iteration number, for manual (picked) and cross-correlation data of relocated earthquakes. The relocation is stable at an rms of 0.1. Four sets of iterations, each with a different weighting criteria, were used, after the method of *Waldhauser and Ellsworth* (2000).

be relocated in three dimensions. Events not relocated are indicated by an asterisk in Table 2.1. Selection of an absolute starting depth for the earthquakes is discussed in the following section.

### 2.3. Relocations and Analysis

Locations of closely spaced earthquakes can be considered in terms of the absolute location of each event, or the relative distances between pairs of events. The uncertainties ( $\text{RMS} < 0.1$ ) from double-difference location reflect uncertainties in the relative inter-event distances. Absolute hypoDD locations (depths in particular) include uncertainty and bias due to station coverage, use of a 1-D velocity model,

and starting location. To address this, we used the locations of *Tréhu et al.* (2008) and two of our own independent locations to determine a realistic average starting depth, and then ran hypoDD to obtain relative location between events.

### 2.3.1 Absolute cluster depth location

The accuracy of absolute depths of earthquakes produced by seismic networks in this area is difficult to determine, due to the fact that a single 1-D velocity model does not accurately represent the velocity structure at a regional scale. Geological features, including the subducting plate itself, the lateral contrast in mid-crustal velocity between accreted sediments and the Siletz terrane, and the variable thickness of basin sediments, are not well-represented by a flat-layer model.

*Tréhu et al.* (2008) located the two largest events using teleseismic pP and local PmP arrivals. By raytracing PmP and pP paths through a 2-D model obtained from active source seismic data (*Tréhu et al.*, 1994; *Gerdomeo et al.*, 2000), they determined a well-constrained depth of 16 km for the 08/19/04 earthquake. Teleseismic pP arrival times were used to locate the 07/12/04 event at a depth of 9-11 km, which is less well-constrained because the event occurred south of the active source line, and no PmP phases were readily observed. These depths for the July and August events are 15 and 10 km shallower, respectively, than the 26 km average depth of the clusters as located by PNSN.

### 2.3.2 Location of two earthquakes with COLZA stations

We deployed an onshore/offshore seismic array, beginning in September 2007, to better observe earthquakes offshore central Oregon. The array consisted of 6 onshore seismic stations from the USArray FlexArray, as well as two one-year-long deployments of (15 and 18) ocean-bottom seismometers (OBS) from the Ocean Bot-

tom Seismograph Instrument Pool (OBSIP). Instrument coordinates and recording time periods for the stations used for relocation are listed in Table 2.2. (All stations are shown in Figure 2.1.)

Two earthquakes in the southern cluster were recorded by this network on 29 April ( $M_c$  2.1) and 1 May 2008 ( $M_c$  2.9). In order to verify the *Tréhu et al.* (2008) conclusion that the hypocenters in this cluster were located much shallower than indicated by the regional networks, we located these two events independently using stations that were closest to the event (inverted triangles in Figure 2.1) and a velocity model (described below) that best represented the structure between the earthquakes and the close-by stations. To maintain a consistent approach, only the five closest stations, which recorded clear P- and S-arrivals for both events, were used in the locations.

In locating these two earthquakes, we used a Levenberg-Marquardt least-squares inversion, implemented in the GENLOC library (*Pavlis et al.*, 2004), using a 1-D travel-time calculator. We repeated the inversion for several velocity models, including the O0 model used by the PNSN for this area, and performed additional tests with slight modifications in the travel time data set to test epicenter and depth sensitivity of the results. For all tests, epicenters were very stable (within 3 km within each other) and depths were generally much shallower than given by PNSN. Figure 2.5 summarizes the results for the O0-model used by PNSN (2.5a) and our preferred model (2.5b), derived from the 2-D velocity model of *Gerdomb et al.* (2000). The O0 model produced depths of  $\sim 22$  km for both events, while the preferred model produced depths of 13 and 16 km, which are  $\sim 19$  km shallower than the catalog depths reported by the PNSN. The results for these two events reinforce the shallower depth determined by *Tréhu et al.* (2008) for the main 07/12/04

southern cluster event. Given the northern cluster earthquake depth of 16 km from *Tréhu et al. (2008)* and the southern cluster earthquake depths of 13 and 16 km, we seeded the hypoDD runs with initial starting epicenters as reported in the catalogs and all starting depths set to 15 km.

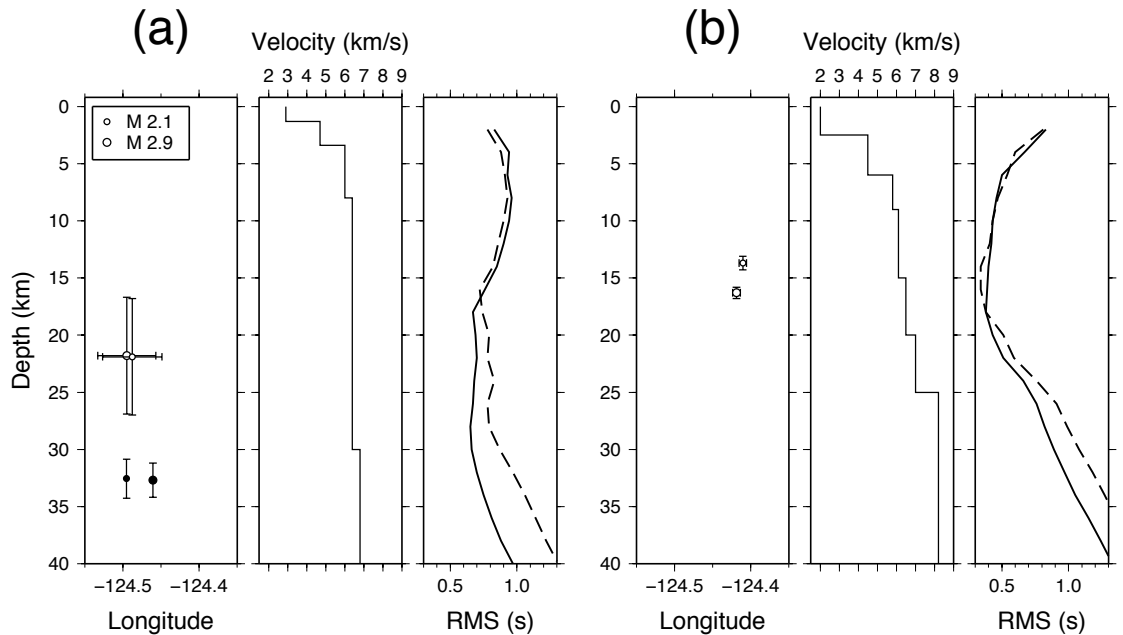


FIGURE 2.5: Locations (white circles) of the 29 April 2008 (M 2.1) and 1 May 2008 (M 2.9) events with onshore/offshore COLZA stations, using (a) the general offshore velocity model used by PNSN, and (b) an offshore velocity model derived from *Gerdorn et al. (2000)*. The amphibious network locates the earthquakes at a depth of  $\sim 15$  km using the model in (b), and the uncertainties are greatly reduced using this more realistic model. The rms residual for our arrival-time dataset, calculated for fixed-depth locations at 2 km depth intervals, is plotted for both models (solid line is the May event; dotted line is the April event). In model (a), from 17 to 30 km, rms minima are not well defined. Using the same dataset, model (b) shows clear rms minima for both events, with values decreased by  $\sim 40\%$  from model (a). Error bars for events located in this paper are maximum velocity model uncertainty after *Pavlis (1986)*. Black circles in (a) are the original PNSN catalog locations, with corresponding error bars.

### 2.3.3 Relative Relocations

Double-difference relocation confirms that the earthquakes occurred in distinct clusters around the two largest events (Figure 2.6). The northern cluster, at  $\sim 44.6^\circ\text{N}$ , appears to be split into two separate subsets, with the main 08/19/04 event and three immediate aftershocks occurring  $\sim 5$  km north-northeast of the tightly clustered group of 2003, 2006, and 2007 events. The three 2006 earthquakes were not originally detected by the PNSN, and the ANF catalog epicenters (the three easternmost events south of  $44.5^\circ\text{N}$  in Figure 2.6) are  $\sim 25$  km southeast of their relocated epicenters. The southern cluster, at  $\sim 44.3^\circ\text{N}$ , remains slightly elongated and more dispersed. This is consistent with the waveform data as seen in Figure 2.3, where waveforms from southern cluster events show more variability, including S-P amplitude ratios. Thus, we would expect southern cluster earthquakes to be somewhat separated in space and/or to have different source mechanisms.

In terms of epicenter, the absolute locations of the two 2008 events from this paper are consistent with the eastern shift of the hypoDD relocations of the southern cluster relative to the catalog locations. Both events were relocated  $\sim 5$  km east of their locations as determined by the PNSN network. Due to the larger azimuthal gap and lower number of nearby stations for the southern cluster, we would expect the longitudinal component of the epicenters to be the least well-constrained in the catalog locations.

The new hypocenter distribution decreases the depth range significantly within each cluster; events are located within a  $\sim 3$  km vertical range and define a landward-dipping plane (Figure 2.7). The epicenter of the 08/19/04  $M_w$  4.7 event does not change significantly; however, the southern 07/12/04 event is shifted to the east.

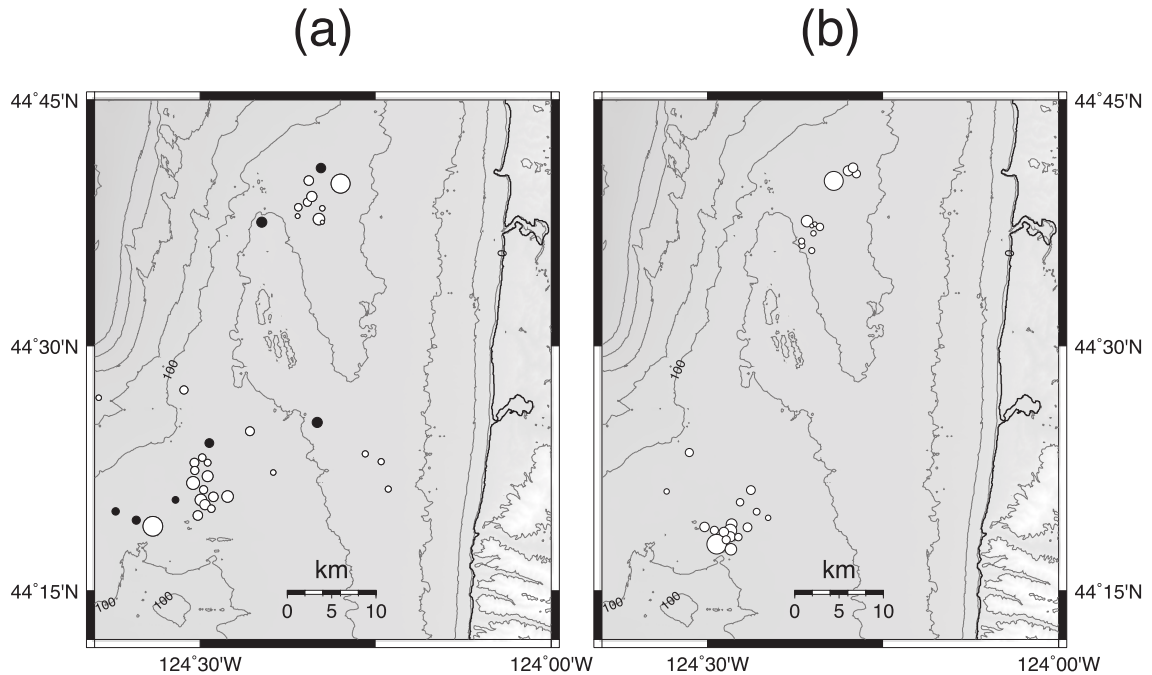


FIGURE 2.6: (a) Before and (b) after epicenter maps of the relative relocations. Events are more tightly clustered after relocation. Subclusters within the northern cluster are a stable result and are consistent with subclustering indicated by waveform cross-correlation in Figure 2.3. Black circles are events not relocated (by hypoDD) due to lack of a sufficient number of nearby event pairs.

In order to test the robustness of the relative event clustering, we performed relocations at alternate starting depths of 5, 10, 20 and 25 km. These results are summarized in Figure 2.7c. For shallower starting depths of 5 and 10 km, an increasing number of “airquakes” are located above the seafloor and discarded in the relocation process. At deeper starting depths of 20 and 25 km, the higher velocities of the subducting plate cause events to diverge away from each other and locate outside of the clusters, thus reducing the number of relocated events. The overall shape of the clusters is similar to those using a 15 km starting depth, but the absolute location is deeper, confirming that hypoDD depths are biased by the starting configuration. During multiple runs, the most consistent and tightly

clustered results were at a starting depth of 15 km. This is expected, as the local velocity between events should be the most accurate at the true earthquake depth.

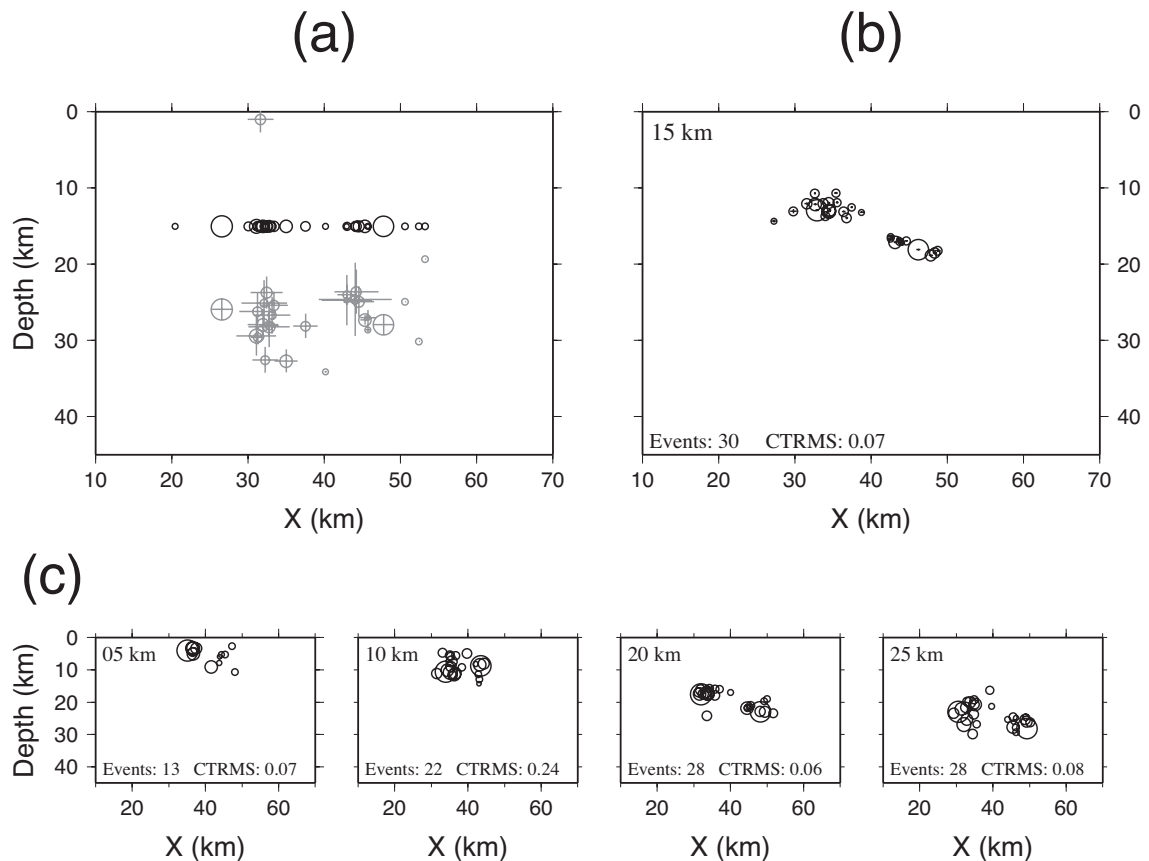


FIGURE 2.7: Depth relocations, in a west-to-east cross-section, showing (a) original and (b) relocated hypocenters using a starting depth of 15 km. Error bars in (a) are given catalog uncertainties; error bars in (b) are as calculated by hypoDD (most are smaller than the symbol width). (c) Results of relative relocations using alternate starting depths, with number of events and relative rms of the catalog data. Shallower starting depths result in increasing numbers of events located above ground and discarded. Deeper starting depths result in divergence (and discarding) of events from the cluster due to the increased velocity at those depths. The largest number of events is retained, and the earthquakes are most closely clustered for our preferred starting depth of 15 km. X axis is UTM easting shifted by -350 km.

## 2.4. Discussion

Figure 2.8 shows relocated hypocenters from this paper superimposed on the velocity model determined by *Gerdom et al.* (2000). The northern cluster, which occurred at the latitude of the velocity model, is directly located over a “bright spot” of strong reflectivity on the plate boundary, which *Gerdom et al.* (2000) interpret as an area of high fluid content due to a metamorphic facies transition. The presence of fluids trapped at the plate interface may explain the increased seismicity in this spot; however, a similar “bright spot” observed by *Tréhu et al.* (1994, 1995) about 25 km north of the *Gerdom et al.* (2000) line (see Figure 2.1) produces no earthquake activity.

The southern cluster also appears on or near the plate boundary in Figure 2.8, although the along-strike extension of this velocity model to the south is approximate, and the plate boundary reflectivity here is unknown. Current data are not adequate to evaluate whether the “bright spot” observed further north is laterally continuous and present at the southern cluster location. *Tréhu et al.* (A. M. Tréhu, R. J. Blakely, and M. C. Williams, in review, 2011) associate these southern cluster earthquakes with a collision between a subducted seamount on the Juan de Fuca plate with crystalline rocks of the Siletz terrane. Topographic features on the downgoing plate have been identified at various stages of subduction at convergent margins around the world (*Fleming and Tréhu*, 1999; *Kodaira et al.*, 2000; *Husen et al.*, 2002; *Watts et al.*, 2010). However, the mechanism of how they affect earthquake rupture is not well understood, and may differ from zone to zone (*Cummins et al.*, 2002; *Watts et al.*, 2010). In a frictional model of long-term rupture cycles at Nankai, which included a known subducted seamount imaged by active

source seismic work, *Kodaira et al.* (2006) found that the frictional properties of the seamount affected the propagation of rupture over multiple earthquake cycles. Their model produced small earthquakes and/or slow slip adjacent to the seamount before a full rupture. In Cascadia, segmented rupture could similarly be affected by subducted features on the plate interface, which may conditionally impede or allow a through-going large earthquake rupture.

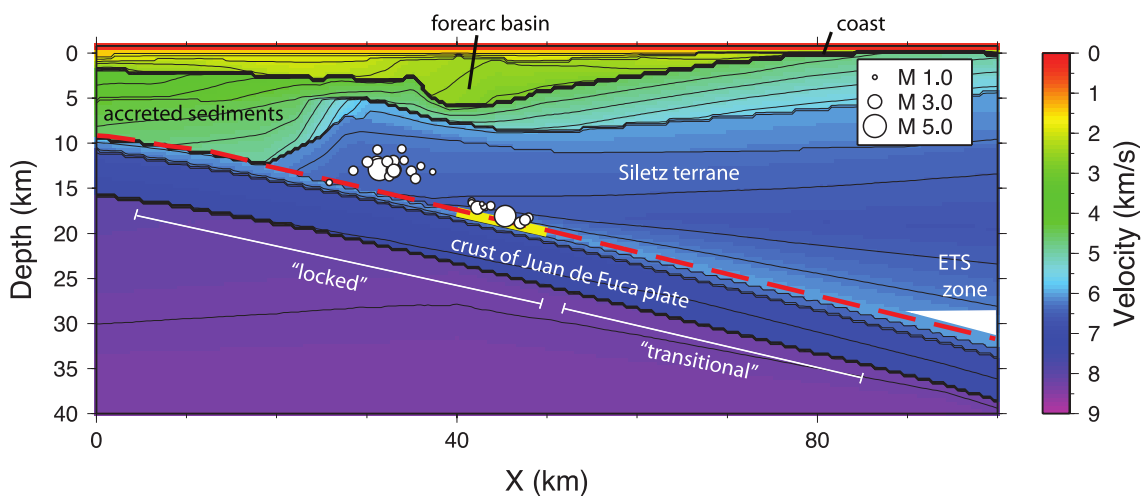


FIGURE 2.8: Final event locations superimposed on the *Gerdom et al.* (2000) velocity model, which corresponds to the latitude of the northern (downdip) cluster. This cluster occurs on the plate boundary (dashed line) at a highly reflective area (yellow line), identified from the active seismic survey by *Gerdom et al.* (2000). Approximate extent of the nominally locked, transitional, and episodic tremor and slip sections of the plate boundary are also indicated for reference. X axis is UTM easting shifted by -350 km.

The earthquakes in this study occurred at one of the segment boundaries proposed for this margin based on paleoseismic (*Goldfinger et al.*, 2008) and potential field (*Wells et al.*, 2003) studies, and may therefore provide insight to understanding rupture propagation in Cascadia during a great megathrust earthquake. Correlation of paleohistoric evidence of co-seismic subsidence, tsunami inundation (*Nelson et al.*, 2006), and offshore turbidites (*Goldfinger et al.*, 2008) produce different earthquake

records for the Washington/Northern Oregon and Southern Oregon/California parts of the subduction zone. *Goldfinger et al.* (2008) posit several partial rupture areas. Their approximate boundary separating a long segment to the north and multiple segments to the south occurs at  $44.5^{\circ}\text{N}$ , midway between the two clusters in this study. Over half of their partial-rupture events appear not to have propagated northward past this point. *Wells et al.* (2003) have proposed a correlation between segmentation of slip along subduction zone margins and forearc basin structure, as evidenced by gravity lows. In Cascadia there are no modern rupture limits to compare to structure; however, the earthquakes in this study occurred on a gravity high located between two major forearc gravity lows (*Wells et al.*, 2003). Slip deficit models obtained from inversion of regional GPS data by *McCaffrey et al.* (2007) reveal an along-strike change in slip deficit at  $\sim 44.5^{\circ}\text{N}$ , which is more marked in models with less along-strike smoothing.

Interface earthquakes in the “locked” or “transitional” parts of the subduction zone are rarely seen in central Cascadia. There are only two other cases of low-angle thrust events of moderate magnitude potentially located on the megathrust. One occurred in 1996, off of Cape Blanco, near  $42.5^{\circ}\text{N}$  (*J. Nabelek and J. Braunmiller*, unpublished) and the other in 2008, near  $41^{\circ}\text{N}$  (UC Berkeley Moment Tensor Catalog, see Data and Resources). As seen in Figure 2.2, there has been persistent earthquake activity (several events per year) at these two clusters near  $44.5^{\circ}\text{N}$  offshore central Oregon since 2003. This area of the subduction zone is unique in Cascadia, having seismicity on the plate boundary in a region that divides segments of the subduction zone with different earthquake histories, gravity signatures, and apparent degrees of plate coupling.

## 2.5. Conclusions

The relocation of the micro-seismicity at  $\sim 44.5^\circ\text{N}$  at the locked zone in Cascadia suggests that seismic slip is occurring in small concentrated areas, or “patches” on or above the plate boundary, not in the Juan de Fuca mantle as indicated by regional catalog locations. Due to the sparse station coverage, the asymmetry of crustal structure in the region, and the use of simplified velocity models for regional network locations, there is a systematic bias in the location of offshore subduction zone earthquakes by regional networks. Our locations are on average 13 km shallower in depth. In terms of epicenter, the largest uncertainty is perpendicular (longitudinal) to the coast due to the geometry of seismic stations: the farther offshore the earthquake, the more uncertain its epicentral location. While the epicentral uncertainty for the northern cluster is small, on the order of a few kilometers, uncertainty for the southern cluster is likely greater; our absolute locations using OBS data were  $> 5$  km southeast of the original cluster location.

The proximity of the earthquakes to the plate boundary, as well as the source mechanisms of the two largest quakes, suggest they most likely represent seismicity on the megathrust plate interface. The rarity of interface earthquakes in Cascadia makes these events significant, since they provide further evidence for plate boundary heterogeneities near proposed partial rupture limits for great Cascadia earthquakes.

## 2.6. Data and Resources

Earthquake catalogs were obtained from the Pacific Northwest Seismic Network ([www.pnsn.org/CATDAT/catalog.html](http://www.pnsn.org/CATDAT/catalog.html)). EarthScope Array Network Facility events were obtained by personal communication, but catalogs are available (<http://anf.ucsd.edu/tools/events/download.php>). Seismograms were obtained from the IRIS Data Management Center at [www.iris.edu](http://www.iris.edu). Seismograms were also collected as part of the COLZA experiment (IRIS network code XA2008-2009), using EarthScope FlexArray PASSCAL instruments; these data will become available in mid-2011 from the IRIS DMC. Seismic data were processed using the PASSOFT software developed and made available by PASSCAL (<ftp://ftp.passcal.nmt.edu/passcal/software/>). For further processing, we used Antelope software from Boulder Real Time Technologies, contributed software and libraries from the Antelope Users Group ([www.indiana.edu/~aug/](http://www.indiana.edu/~aug/)), and the MATLAB object toolboxes developed by Celso Reyes and Michael West available from the Geophysical Institute of the Alaska Volcano Observatory ([www.giseis.alaska.edu/Seis/EQ/tools/GISMO/](http://www.giseis.alaska.edu/Seis/EQ/tools/GISMO/)) The Moment Tensor Catalog of the Berkeley Seismological Laboratory is available (<http://seismo.berkeley.edu>). Some figures were made using the Generic Mapping Tools, version 4.5 (*Wessel and Smith, 1998*).

## 2.7. Acknowledgements

The COLZA array was funded by a grant from the U.S. National Science Foundation (NSF-OCE050402) and used instruments from the EarthScope FlexArray and the Ocean Bottom Seismometer Instrument Pool. Additional funding was

provided by NSF-OCE0752598. We would like to thank the staff at PASSCAL and the L-CHEAPO OBSIP team at the Scripps Institution of Oceanography for their work and assistance in deploying and maintaining the seismic network equipment in the field, as well as the captain and crew of the R/V *Wecoma*.

### 3. CONCLUSIONS

In addition to the inherent value of containing more accurate locations of the earthquakes themselves, the results of this manuscript produce several conclusions related to earthquake study in Cascadia, which are further discussed in the following sections.

#### 3.1. Suitability of the hazard earthquake catalog for offshore scientific research

The earthquake catalogs produced by the regional networks for the offshore area of Cascadia lack the accuracy needed to study offshore faults. Offshore stations and a more accurate velocity model can improve the catalog significantly. Additionally, incorporating double-difference relocation into an automatic process, as has been tested in California (*Waldhauser, 2009*), would not only make offshore historical catalogs much more useful in seismological research, but also improve the accuracy of new locations.

#### 3.2. Co-located static and kinematic evidence for frictional anomalies

The new locations indicate that the earthquakes cluster tightly in spots on the subducting plate interface. One cluster occurs at a spot of strong reflectivity on the plate. The other occurs adjacent to a proposed subducted seamount (*A. M.*

*Tréhu, R. J. Blakely, and M. C. Williams*, in review, 2011). Both of these spots are now sites which exhibit structural (based on seismic and magnetic imaging) and behavioral (based on the earthquakes) evidence of frictional anomalies.

### **3.3. Possible implications for rupture segmentation**

The sheer area that must be displaced to produce an earthquake of magnitude 9 sometimes requires that slip occur on more than one large seismic asperity. Whether multiple asperities repeatedly slip simultaneously over multiple seismic cycles is another uncertainty in the study of megathrust earthquakes, and has made such events extremely difficult to forecast.

While no large earthquake has been recorded on modern sensors in Cascadia, there have been several magnitude 9 earthquakes recorded at other subduction zones within the past century. Identifying analogous or similar frictional anomalies at these other megathrust boundaries and noting their effect on rupture propagation may provide insight on how these anomalies will affect a Cascadia rupture.

Additionally of course, in the event of a full or partial seismic rupture of the Cascadia margin, comparing the location of these clusters to the extent of the rupture, and noting whether or not rupture was slowed or impeded in any way over these frictionally anomalous areas of the plate boundary could provide invaluable clues to the nature of large-scale seismic behavior, in Cascadia and elsewhere.

## BIBLIOGRAPHY

- Adams, J. (1990), Paleoseismicity of the Cascadia subduction zone: Evidence from turbidites off the Oregon-Washington margin, *Tectonics*, *9*(4), 569–583, doi:199010.1029/TC009i004p00569.
- Atwater, B. F. (2005), *The orphan tsunami of 1700: Japanese clues to a parent earthquake in North America*, U.S. Geological Survey.
- Cummins, P. R., T. Baba, S. Kodaira, and Y. Kaneda (2002), The 1946 Nankai earthquake and segmentation of the Nankai Trough, *Physics of The Earth and Planetary Interiors*, *132*(1-3), 75–87, doi:10.1016/S0031-9201(02)00045-6.
- Fleming, S. W., and A. M. Tréhu (1999), Crustal structure beneath the central Oregon convergent margin from potential-field modeling: Evidence for a buried basement ridge in local contact with a seaward dipping backstop, *Journal of Geophysical Research*, *104*(B9), 447.
- Gerdom, M., A. M. Tréhu, E. R. Flueh, and D. Klaeschen (2000), The continental margin off Oregon from seismic investigations, *Tectonophysics*, *329*(1-4), 79–97, doi:10.1016/S0040-1951(00)00190-6.
- Goldfinger, C., C. H. Nelson, and J. E. Johnson (2003), Holocene earthquake records from the Cascadia subduction zone and Northern San Andreas Fault based on precise dating of offshore turbidites, *Annual Review of Earth and Planetary Sciences*, *31*(1), 555–577, doi:10.1146/annurev.earth.31.100901.141246.
- Goldfinger, C., et al. (2008), Late Holocene rupture of the Northern San Andreas

- Fault and possible stress linkage to the Cascadia subduction zone, *Bulletin of the Seismological Society of America*, *98*(2), 861–889, doi:10.1785/0120060411.
- Husen, S., E. Kissling, and R. Quintero (2002), Tomographic evidence for a subducted seamount beneath the Gulf of Nicoya, Costa Rica: The cause of the 1990 Mw = 7.0 Gulf of Nicoya earthquake, *Geophysical Research Letters*, *29*(8), 10.1029/2001GL014,045.
- Kodaira, S., N. Takahashi, A. Nakanishi, S. Miura, and Y. Kaneda (2000), Subducted seamount imaged in the rupture zone of the 1946 Nankaido earthquake, *Science*, *289*(5476), 104–106, doi:10.1126/science.289.5476.104.
- Kodaira, S., T. Hori, A. Ito, S. Miura, G. Fujie, J. Park, T. Baba, H. Sakaguchi, and Y. Kaneda (2006), A cause of rupture segmentation and synchronization in the Nankai trough revealed by seismic imaging and numerical simulation, *Journal of Geophysical Research*, *111*, 17, doi:200610.1029/2005JB004030.
- Leonard, L. J., R. D. Hyndman, and S. Mazzotti (2003), Coseismic subsidence in the 1700 great Cascadia earthquake: Coastal estimates versus elastic dislocation models, *Geological Society of America Bulletin*, *116*(5-6), 655–670, doi:10.1130/B25369.1.
- McCaffrey, R., A. I. Qamar, R. W. King, R. Wells, G. Khazaradze, C. A. Williams, C. W. Stevens, J. J. Vollick, and P. C. Zwick (2007), Fault locking, block rotation and crustal deformation in the Pacific Northwest, *Geophysical Journal International*, *169*(3), 1315–1340, doi:10.1111/j.1365-246X.2007.03371.x.
- Nelson, A. R., H. M. Kelsey, and R. C. Witter (2006), Great earthquakes of variable

- magnitude at the Cascadia subduction zone, *Quaternary Research*, *65*(3), 354–365, doi:10.1016/j.yqres.2006.02.009.
- Pavlis, G. L. (1986), Appraising earthquake hypocenter location errors: A complete, practical approach for single-event locations, *Bulletin of the Seismological Society of America*, *76*(6), 1699–1717.
- Pavlis, G. L., F. Vernon, D. Harvey, and D. Quinlan (2004), The generalized earthquake-location (GENLOC) package: an earthquake-location library, *Computers & Geosciences*, *30*(9-10), 1079–1091, doi:10.1016/j.cageo.2004.06.010.
- Satake, K., K. Wang, and B. F. Atwater (2003), Fault slip and seismic moment of the 1700 Cascadia earthquake inferred from Japanese tsunami descriptions, *Journal of Geophysical Research*, *108*(B11), 2535, doi:10.1029/2003JB002521.
- Tréhu, A. M., I. Asudeh, T. M. Brocher, J. H. Luetgert, W. D. Mooney, J. L. Nabelek, and Y. Nakamura (1994), Crustal architecture of the Cascadia forearc, *Science*, *266*(5183), 237–243, doi:10.1126/science.266.5183.237.
- Tréhu, A. M., G. Lin, E. Maxwell, and C. Goldfinger (1995), A seismic reflection profile across the Cascadia subduction zone offshore central Oregon: New constraints on methane distribution and crustal structure, *Journal of Geophysical Research*, *100*(B8), 116.
- Tréhu, A. M., J. Braunmiller, and J. L. Nabelek (2008), Probable low-angle thrust earthquakes on the Juan de Fuca-North America plate boundary, *Geology*, *36*(2), 127–130, doi:10.1130/G24145A.1.

- Waldhauser, F. (2009), Near-Real-Time Double-Difference event location using long-term seismic archives, with application to Northern California, *Bulletin of the Seismological Society of America*, *99*(5), 2736–2748, doi:10.1785/0120080294.
- Waldhauser, F., and W. L. Ellsworth (2000), A Double-Difference earthquake location algorithm: Method and application to the Northern Hayward Fault, California, *Bulletin of the Seismological Society of America*, *90*(6), 1353–1368, doi:10.1785/0120000006.
- Watts, A. B., A. A. P. Koppers, and D. P. Robinson (2010), Seamount subduction and earthquakes, *Oceanography*, *23*(1), 166–173.
- Wells, R. E., R. J. Blakely, Y. Sugiyama, D. W. Scholl, and P. A. Dinterman (2003), Basin-centered asperities in great subduction zone earthquakes: A link between slip, subsidence, and subduction erosion?, *Journal of Geophysical Research*, *108*, 30, doi:200310.1029/2002JB002072.
- Wessel, P., and W. H. F. Smith (1998), New, improved version of generic mapping tools released, *Eos*, *79*(47), 579.

